MRS Advances © 2015 Materials Research Society
DOI: 10.1557/adv.2015.23

Hierarchically Self-assembled Super Structural TiO_2 Microspheres: Enhanced Excitonic Efficiency as Photocatalyst and Photoanode Material

Arunkumar Shanmugasundaram, Pratyay Basak, and Sunkara V. Manorama*
Nanomaterials Laboratory, Inorganic and Physical Chemistry Division,
CSIR-Indian Institute of Chemical Technology, Hyderabad 500007, India.

ABSTRACT

Complex three-dimensional (3-D) super structural TiO_2 architectures with controlled shape and size were synthesized by a facile hydrothermal synthesis route by using titanium tetrachloride ($TiCl_4$) as the metal precursor and hydrochloric acid (HCl)/ammonium chloride (NH_4Cl) as the mineralizer/structure directing agent. Several interesting hierarchical architectures *like:* (*i*) nanoparticles assembled spheres (*NPAS*), *(ii)* nanowires assembled spheres (*NWAS*), *(iii)* nanorods assembled spheres (*NRAS*), and *(iv)* nanosheets assembled spheres (*NSAS*) were achieved by the controlled variation of crystal structure modifier. The synthesized materials were characterised in detail by different analytical techniques and the findings are consistent. To demonstrate the superior performances of the as prepared materials the photocatalytic and photo-voltaic performances were investigated. The results demonstrate that these synthesized materials exhibits enhanced photocatalytic activity (efficiency is ~ 91%) towards the degradation of RhB and as a photoanode in DSSCs the maximum energy conversion efficiency is ~5%, attributed primarily to the unique hierarchical mesoporous structure of the TiO_2 architectures.

INTRODUCTION

Owing to its unique *physico-chemical* and *opto-electronic* properties TiO_2 is considered as, one of the most important metal oxide semiconductors and its potential has been suitably demonstrated in several applications [1]. Over the years several form of TiO_2 hierarchical architectures have been reported. However, the development of facile and effective methods for creating novel super structural architectures which can perform better than the existing materials is a topic of research and remains a great challenge for the materials scientists [2]. Herein, we demonstrate in detail the preparation of 3-D hierarchical rutile TiO_2 architectures with controlled morphologies through a facile hydrothermal synthesis method notably without use of any surfactant or template. The morphological and crystal structure evaluations of the synthesized materials were characterized extensively. The as-prepared TiO_2 architectures were used as the photocatalyst for the degradation of Rhodamine-B (RhB) and photo anode for dye sensitized solar cells.

EXPERIMENT

Preparation of hierarchical mesoporous TiO_2 architectures

In a typical synthesis procedure, 0.25 M of $TiCl_4$ (25% $TiCl_4$ in HCl) solution was added to 20 mL of cold water, followed by the addition of 2.5 M of HCl to the above mentioned solution. After 15 min of stirring, 1.5 mM of NH_4Cl was added to the above solution to get the

desired reactant mixture. The mixture was transferred into a Teflon lined stainless steel autoclave, maintained at 150 ^{o}C for 12 and the resultant products were collected by centrifugation. Other TiO_2 architectures were synthesized similarly except varying the concentration of HCl/NH_4Cl in the reaction medium. The reaction conditions and corresponding TiO_2 morphology are summarized in Table 1.

Table 1. Reaction conditions and corresponding TiO_2 morphology

Sample code	$TiCl_4$ (M)	HCl / NH_4Cl molar ratio	Morphology
NPAS	0.25	2.5/1.5	Nanospheres assembled spheres
NWAS	0.25	5.0/1.5	Nanowires assembled spheres
NRAS	0.25	2.5/3.0	Nanorods assembled spheres
NSAS	0.25	2.5/4.5	Nanosheets assembled spheres

RESULTS AND DISCUSSION

Morphological and crystal structure analysis

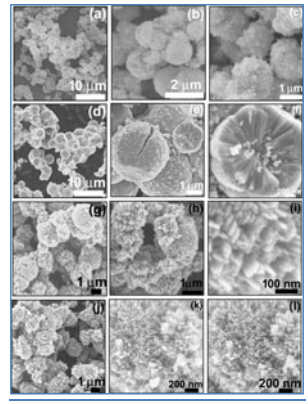

Figure 1. FE-SEM images of as prepared rutile-TiO_2 hierarchical architectures at different magnifications; **(a-c)** spheres assembled micron spheres; **(d-f)** nanowires assembled spheres; **(g-i)** nanorods assembled spheres; **(j-l)** nanosheets assembled spheres.

Figure 1 shows the typical FESEM images of the as prepared samples. When ratio of HCl:NH_4Cl is maintained as 2.5:1.5 M, nearly uniform sized microspheres with an average diameter of 1.5 μm are observed (Figure 1(a)). Higher magnification micrograph (Figure 1(b, c)), reveals structures that are composed of large number of closely packed nanospheres of size 200 nm. On increasing the HCl concentration further in the reaction medium, *i.e.* 5:1.5 ratio, micron sized spheres of larger size ~2-3 μm are obtained (Figure 1(d)). Closer observation of the fractured microsphere (Figure 1(e, f)) reveals the densely packed ultrafine nanowires of size ~5-10 nm that are the building blocks of the spheres. This observation leads us to believe that the

microspheres were formed by radial growth of TiO_2 nanowires on the initial nuclei (nanoparticulate core). When the concentration of the NH_4Cl in the reaction medium, is increased (2.5:3) ratio nanorods assemble to form flower-like spherical morphologies of size ~2 μm. (Figure 2(g)). In the magnified image (Figure 1(h, i)) one can clearly observe that these spheres are aggregated assemblies of the nanorod bundles and each of these bundles comprise of several thinner nanorods bunched together. Further increasing the concentration of NH_4Cl (2.5:4.5) nanosheets assembled sphere-like morphology of size ~2 μm are clearly observed (Figure 1(j-l)) where the nanosheets are of size ~200 nm. The detailed crystal growth formation mechanism and the role of the reaction parameters such as reaction medium, time, temperature and HCl, NH_4Cl on the formation of these exotic hierarchical architectures are under investigation.

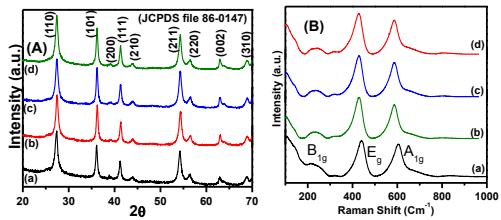

Figure 2. (A) Powder Xray diffraction pattern and **(B)** Micro-Raman spectroscopy analysis of the as prepared mesoporous hierarchical TiO_2 architectures samples: **(a)** nanospheres assembled spheres, **(b)** nanowire assembled spheres, **(c)** nanorods assembled spheres and **(d)** nanosheets assembled spheres.

Table 2. The physical parameters of the as synthesized samples.

Sample Code	Crystallite size (nm)	Lattice parameters		BET surface area (m^2g^{-1})	Pore diameter (nm)	Band gap (E_g)
		a = b nm	C = nm			
NPAS	11.2	0.459	0.295	66	2.130	3.1
NWAS	9.1	0.455	0.291	88	6.722	3.03
NRAS	10.7	0.458	0.293	77	2. 244	3.05
NSAS	11.6	0.459	0.295	69	2.012	3.08

The crystal structure and phase purity of the final products were carried out by powder X-ray diffraction (XRD) and micro-Raman analysis. All the diffraction patterns (Figure. 1A) can be perfectly indexed to the tetragonal phase of rutile TiO_2, with the space group $P4_2/mnm$ (136) (JCPDS file 86-0147). The calculated lattice parameters (Table. 2) exactly match with the reported value of rutile-TiO_2 [3]. The room temperature Raman spectra (Figure. 1B) clearly reveals the Raman bands at 242, 446, and 610 cm^{-1} which can be assigned to the B_{1g}, E_g, and A_{1g} modes of rutile TiO_2. The Raman shift at 446 cm^{-1} corresponds to the oxygen vibrational mode and the Raman shift at 610 cm^{-1} can be assigned to the stretching vibrational mode of the Ti–O bond. The Raman shift at 242 cm^{-1} can be assigned to a second-order phonon [4]. The optical band gaps of the as prepared samples are studied by UV-DRS analysis (not shown) in the % reflectance mode. The calculated band gaps (Table 2) vary slightly with the morphology which can be attributed to the difference in the constituent particle size. The surface area and pore size distribution were determined by the N_2 adsorption-desorption isotherms method which reveals a

type IV isotherm indicating the mesoporous nature of the materials. The calculated BET surface area and the corresponding pore diameter for the as synthesized samples are presented in Table 2.

Photocatalytic efficiency of TiO_2 architectures

Of all water contaminants, organic dyes one of the major pollutants causing imbalance in the ecosystem, get accumulated, stored and transferred through various organisms and/or up the food chain and hence, their elimination from water bodies remains a challenge to be addressed. In this context materials that can either selectively absorb or degrade these toxins efficiently can provide effective environmental remediation. Materials with considerable porosity and high surface area combined with appropriate optical band gap are expected to promote photocatalytic reaction on their surfaces. In an effort to exploit the envisaged superior photocatalytic activities of these hierarchically assembled titania superstructures, decomposition of Rhodamine B as model system under visible light is showcased.

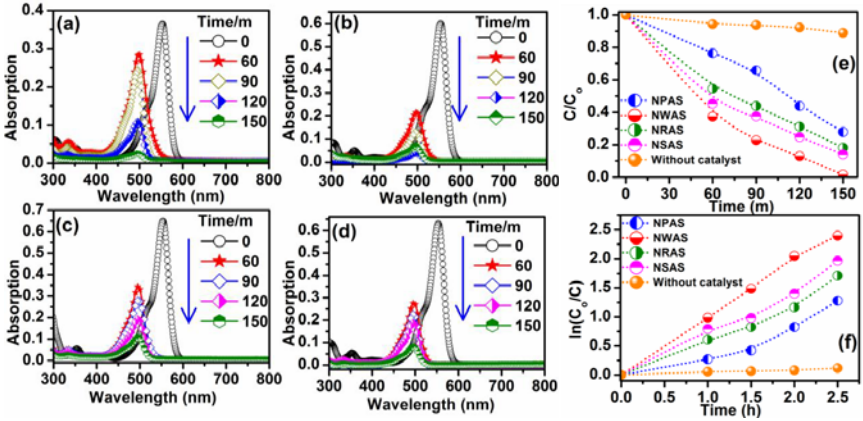

Figure 3. UV−visible absorbance spectra depicting the change in concentration of the dye, RhB solution in the presence of TiO_2 under visible light irradiation as a function of time. **(a)** nanospheres assembled spheres, **(b)** nanowire assembled spheres, **(c)** nanorods assembled spheres and **(d)** nanosheets assembled spheres, (e) Normalized photocatalytic degradation of RhB as a function of time with and without catalyst under light, (d) Estimation of rate constants from the linear fits to the experimental data.

The photocatalytic performance and efficiency of the as prepared materials was evaluated under visible light illuminations. In a typical photocatalytic reaction 0.02 g of synthesized TiO_2 was ultrasonically dispersed in 20 mL of aqueous RhB (1 x 10^{-5} M) in a quartz reactor. The solution containing the photocatalyst was magnetically stirred for 30 minutes in dark to equilibriate the adsorption/desorption of RhB on the catalyst. Following this the suspension was irradiated with visible light under stirring conditions. 3mL of aliquots was drawn at regular time intervals and centrifuged to obtain a clear supernatant aqueous solution. Absorbance of the supernatant was recorded on a UV-Visible spectrometer at λ_{max} = 500 nm to assess the dye

concentrations post exposure at different time intervals. Figure 3 presents the progressive degradation of RhB on the synthesized materials as a function of visible light illumination time. At sufficiently low concentration of the substrate, the photo degradation process of RhB can be approximated to Langmuir−Hinshelwood first order kinetics. This is expressed as follows: $\ln(C_0/C) = kt$, where C_0 is the initial concentration of the reactant, C is the concentration after a time (t) of the degradation process, and k is the first order rate constant. Figure 3 depicts the reaction kinetics of RhB photocatalytic degradation to estimate the rate of the reaction. After 2.5 h of visible light illumination, the conversion of RhB was 73.2%, 90.9%, 82.1%, and 86% for *(i)* nanoparticles assembled spheres (NPAS), *(ii)* nanowires bunched spheres (NWAS), *(iii)* nanorods assembled spheres (NRAS) and *(iv)* spheres constituting nanosheets (NSAS), respectively.

Photovoltaic Performances

Photo anodes play a major role in enhancing the overall conversion efficiency of dye sensitized solar cells (DSSCs) and tremendous efforts have been devoted to the development of highly effective photo anodes with high specific surface area, fast electron transport, and pronounced light-scattering effects. The hierarchical TiO_2 architectures achieved in this work also holds promise as excellent photoanodes owing to the high porosity, large specific surface area and capability of multiple scattering that translates into higher conversion. Hence, preliminary evaluations of the synthesized hierarchical titania structures were carried out by fabricating DSSC test cells. Dye-sensitized solar cells (DSSCs), a third generation excitonic energy conversion device is considered to be one of the promising photovoltaic devices for the next generation renewable energy mix. The schematic of the DSSC assembly, protocols used for fabrication of the test cell, and measurement setup have been described extensively in earlier works [5]. To evaluate the test-cell efficiency, photoanodes (working electrode) were prepared with pastes of hierarchical TiO_2 architecture. The films were sensitized with N719 dye for a day, soaked with standard BMII based electrolytes and sandwiched with sputter coated platinum electrode (counter electrode). Current-voltage (*J-V*) measurements (Figure. 4) were acquired under a solar simulator that simulated A.M. 1.5G one sun conditions with a power density of 100 mW/cm^2. The photo-active area for all the test cells were held constant (0.13 cm^2) with the aid of a suitable mask and the thickness of the film was controlled in the range of ~5 μm.

Table 3. Summary of the photovoltaic characteristics of TiO_2 photoanodes.

Morphology	Voc (V)	Jsc (mA/cm^2)	Fill Factor	Efficiency (η)
NPAS	0.81	9.96	57.12	4.01
NWAS	0.83	12.95	58.32	5.00
NRAS	0.81	10.94	57.31	4.76
NSAS	0.80	10.53	57.38	4.32

The enhanced photoactivity of the as prepared TiO_2 materials can be attributed to their high specific surface area and unique hierarchical architectures. High specific surface area of the material provides for more dye adsorption sites, and the hierarchical and porous structure also allows enhanced light-scattering. The porosity also helps in improved electrolyte wetting that

possibly improves charge separation and dye-regeneration dynamics leading to higher photovoltaic performance under light [6].

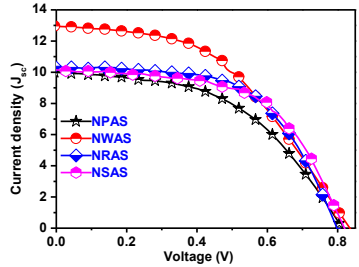

Figure 4. Photovoltaic characteristics of the solid-state DSSC test cells measured under simulated AM 1.5G and one sun condition.

CONCLUSIONS

In summary, we have demonstrated the possibility of synthesizing well-defined 3D-hierarchical rutile TiO_2 architectures with exotic morphologies notably in absence of any surfactant or template as structure directing agent. The as prepared materials were comprehensively characterized employing several analytical techniques that provide important leads to understand the underlying mechanism of nucleation, growth and evolution of these superstructures. The findings evidently highlight the contribution of both Ostwald ripening process and/or oriented attachment mechanism that are involved in the key stages of the formation of these hierarchical architectures. These unique TiO_2 architectures with high porosity and considerably large surface area were showcased and evaluated for visible light photocatalytic activity and performance as efficient photoanodes in model systems.

ACKNOWLEDGEMENTS

All the authors thankfully acknowledge the financial support from CSIR XII plan project M2D (CSC0134) and SVM is also thankful to Department of Science and Technology, India and CICS, Chennai for the International Travel support and financial assistance to attend MRS2015 Fall meeting at Boston, MA, USA.

REFERENCES

1) X. W. Lou, L. A. Archer, Z. C. Yang, *Adv. Mater.* **20**, 3987 **(2008).**
2) H. Zeai, W. Zhouyou, L. Kangle, Z. Yang, D. Kejian, *ACS Appl. Mater. Interfaces*. 5, 8663 **(2013).**
3) J. S. Chen, X. W. Lou, *Chem. Sci.* 2, 2219 (**2011).**
4) H. Cheng, J. Ma, Z. Zhao, L. Qi. *Chem. Mater. 7*, 663 (**1995)**.
5) I. G. Yu, Y. J. Kim, H. J. Kim, C. Lee, W. I. Lee. J. Mater. Chem., 21, 532 **(2011).**
6) Z. Zheng, B. Huang, X. Qin, X. Zhang, Y. Dai, M. Jiang, P. Wang M. H. Whangbo, *Chem. Eur. J.*, 15, 12576 **(2009)**.